

AD-A117 975

MISSION RESEARCH CORP ALBUQUERQUE NM
KMRAD: A LINEARIZED PARTICLE CODE FOR THE STUDY OF RESISTIVE IN--ETC(U)
MAY 82 T P HUGHES, B B GODFREY
AMRC-R-364

F/G 20/9

UNCLASSIFIED

NL

[]
AD
SIC 10

[]



END
DATE
FILMED
69-82
NTIC

AD A117975

12

AMRC-R-364

FINAL TECHNICAL REPORT

KMRAD: A LINEARIZED PARTICLE CODE FOR THE STUDY
OF RESISTIVE INSTABILITIES

T. P. Hughes
B. B. Godfrey

May 1982

Prepared for:

Sandia National Laboratories
Pulse Power Directorate
Albuquerque, New Mexico 87185

Under Contract:

40-0401 (1 Dec 80)
40-0461 (18 Mar 81)

DTIC
ELECTE
AUG 0 6 1982
E

Prepared by:

MISSION RESEARCH CORPORATION
1720 Randolph Road S.E.
Albuquerque, New Mexico 87106

REPRODUCTION IN WHOLE OR IN PART IS PERMITTED FOR ANY PURPOSE
OF THE UNITED STATES GOVERNMENT. APPROVED FOR PUBLIC RELEASE -
DISTRIBUTION UNLIMITED.

82 08 06 046

ABSTRACT

A linearized electromagnetic particle simulation code KMRAD has been developed to look at resistive instabilities on electron beams. The code can simulate three-dimensional dynamics, but by use of Fourier transforms in two directions, only one spatial direction needs to be resolved. For cold beam equilibria, KMRAD predicts growth rates which closely agree with those obtained from an exact cold-fluid code. For a Bennett equilibrium, comparisons between KMRAD and available analytic models are presented, and several discrepancies are noted.



Accession For	
NTIS GRA&I	<input checked="" type="checkbox"/>
DTIC TAB	<input type="checkbox"/>
Unannounced	<input type="checkbox"/>
Justification	
By	
Distribution/	
Availability Codes	
Dist	Avail and/or Special
A	

Portions of this work have already appeared in the form of presentations at scientific meetings and as technical reports [1, 2].

1. T. P. Hughes and B. B. Godfrey, Bull. Am. Phys. Soc. 26, 853 (1981); AMRC-R-325, Mission Research Corporation, Albuquerque, (1981).
2. T. P. Hughes, B. B. Godfrey, C. A. Ekdahl, and R. J. Adler, "Presentation to RADLAC Review," AMRC-R-344, Mission Research Corporation, Albuquerque, (1982).

TABLE OF CONTENTS

<u>Section</u>		<u>Page</u>
	ABSTRACT	i
I.	INTRODUCTION	1
II.	GENERAL INFORMATION ON KMRAD	2
III.	RESISTIVE INSTABILITIES ON BENNETT EQUILIBRIUM BEAMS	6
IV.	STATUS AND FURTHER DEVELOPMENT OF KMRAD	10
	REFERENCES	13

LIST OF ILLUSTRATIONS

Figure		Page
1	Cold beam equilibrium used to test KMRAD. Depicted are radial profiles of the density (n), energy (γ), angular velocity (γV_θ), conductivity (σ), axial and azimuthal magnetic fields (B_z , B_θ). The normalized units correspond to a 10 kA, 50 MeV beam with a radius of 0.9 cm. The beam is 50% current neutralized.	14
2(a)	Radial profiles obtained from KMRAD and GRADR for the $m = 1$ instability. The GRADR mode with maximum growth rate is shown (see Table 1). Only the B_θ , B_r , E_z fields are shown since these are the most important. The solid and dotted lines indicate respectively the real and imaginary parts of each field.	15
2(b)	Radial profiles obtained from KMRAD and GRADR for the $m=2$ resistive instability. See Table 1.	16
3	Comparison of growth rates for the $m = 0$ instability obtained from KMRAD (black rectangles) with those obtained from the analytic models of Lee and Uhm and Lampe. An 80% current neutralization fraction is assumed.	17
4	Radial profiles of the B_θ , B_r , E_z fields for the $m = 0$ mode, obtained from KMRAD. This mode corresponds to the value of k with the largest growth rate shown in Fig. 3.	18
5	Comparison of the (a) real and (b) imaginary parts of the frequency of the $m = 1$ mode obtained from KMRAD, with those obtained from Lee's model. The beam has a Bennett equilibrium with no return current.	19
6	Growth rates of the $m = 1$ instability obtained from KMRAD for $f \geq 0$. We have connected the points for clarity. The dotted line shows results for a broadened conductivity profile.	20
7	Radial profiles of B_θ , B_r , E_z for the $m = 1$ instability at $f = 80\%$, showing that the lowest radial mode is dominant.	21
8	Comparison between the growth rates obtained from KMRAD for the $m = 1$ mode with those obtained from the Uhm-Lampe model. We assume $f = 80\%$.	22

LIST OF ILLUSTRATIONS (Continued)

<u>Figure</u>		<u>Page</u>
9	Growth rates of the $m = 2$ resistive instability computed by KMRAD for various current neutralization fractions. We have connected the points for clarity. There is a weak growth of noise in the code which does not allow us to see where the actual growth rate goes to zero.	23
10	Radial profiles of the B_θ , B_r , E_z fields for the $m = 2$ instability at $f = 0.8$, illustrating the dominance of the lowest radial mode.	24

I. INTRODUCTION

For many applications of intense charged particle beams, the beam must propagate through gases at pressures ranging from one torr to one atmosphere. In this regime, beams are observed to undergo macroscopic disruptions which are thought to be manifestations of resistive instabilities. Since these disruptions are often what determine the distance over which the beam can effectively transport energy, it is important to have a good understanding of resistive instabilities. Those theories presently available¹⁻⁶ make a variety of assumptions which are either unrealistic (e.g., cold beam, step-function radial current profile, etc.) or are founded on plausibility arguments. This rather unsatisfactory state of affairs was the main motivation for developing the linear-theory code KMRAD. In Sec. II, we give a description of KMRAD, and outline the tests to which it has been subjected. In Sec. III, KMRAD is used to obtain the dispersion relations for the $m = 0, 1$, and 2 (m denotes azimuthal mode number) resistive instabilities on intense self-pinched electron beams. Section IV summarizes the status of KMRAD and indicates possible further developments of the code which would increase its usefulness.

II. GENERAL INFORMATION ON KMRAD

A. Description of Code

KMRAD is a linearized,⁷⁻⁹ three-dimensional, fully electromagnetic particle code. The equations which it solves are equivalent to the linearized Vlasov-Maxwell equations. It is written in cylindrical coordinates (r, θ, z) , and can simulate the linear behavior of any plasma system in which the equilibrium is independent of θ and z . KMRAD computes the development of a single Fourier mode (i.e., a perturbation of the form $F(r) \exp(im\theta + ikz)$), given its initial state. Making use of Fourier transforms in this way allows enormous savings in the running time and core requirements of the code, compared to those of a three-spatial-dimensions code. Of course, KMRAD must be run for a range of m and k values to map out a dispersion relation. In practice, however, the number of cases which are of interest is small enough that the Fourier method is still very advantageous.

KMRAD does not generate its own equilibria, and these must therefore be supplied by the user. Any self-consistent equilibrium can be used. To date, we have looked at two specific types of beam equilibrium, (a) a cold-fluid equilibrium with a step-function radial current profile (for testing purposes) and (b) a Bennett equilibrium.

Since we are interested in beam-gas interaction, we need a model for the background gas. In KMRAD, we treat the background as an Ohm's Law medium with a conductivity profile $\sigma(r)$ which is supplied by the user. The profile can be time-varying if desired. The background plasma dynamics are thus incorporated in the equation $\nabla_p = \sigma \underline{E}$, where ∇_p is the plasma current and \underline{E} is the total electric field. An alternative background model is also available in the present version of KMRAD, namely, a cold fluid model.

For diagnostics, KMRAD provides plots of the radial profiles of all components of equilibrium and perturbed fields and currents $E_r, E_\theta, E_z, B_r, B_\theta, B_z, J_r, J_\theta, J_z$. It generates phase-space plots of the equilibrium and perturbed particles (see subsection B). A post-processor is used to provide time histories and power spectra of the fields and currents.

B. Numerical Method: Linearization

The idea of writing linearized particle codes originated some time ago,^{7,8} but has not been widely used. A linearized code is more complicated than a nonlinear code in the following ways. To evaluate the contribution of a single particle to charge and current densities, one must keep track of the particle's unperturbed orbit as well as deviations therefrom produced by perturbed fields. Since the perturbed fields (for the case of a cylindrical beam equilibrium) contain both $\sin(m\theta + kz)$ and $\cos(m\theta + kz)$ components, which are linearly independent, the perturbation of the particle orbit arising from each component must be computed separately. (A simulation particle might be visualized as a cylinder concentric with the beam axis with small helical perturbations, proportional to $\sin(m\theta + kz)$ and $\cos(m\theta + kz)$, on its surface.) Thus, a particle's position and momentum ($\underline{r}, \underline{p}$) is represented by eighteen numbers: six for the equilibrium values and six for both components of the perturbed values. In general, the mathematical expressions in a linearized code are much more lengthy than those of a nonlinear code, just as a result of linearization. The great advantage of linearization comes about when the Vlasov equilibrium one wishes to examine has one or more symmetries, as in the case of a cylindrical beam. For the latter, by using a Fourier representation of the θ and z dependence of perturbations, only the radial dependence needs to be spatially resolved.

C. Numerical Method: Field Solver

To solve the field equations, we employ a time-biasing scheme.¹⁰ This is a numerical method used to beat the Courant restriction on the time step used in the code, while at the same time damping out unphysical high-frequency noise. The method is particularly useful when the frequencies one is trying to simulate are lower than those of light-waves. Time-biasing has been successfully implemented in two-dimensional PIC codes.^{10,11} Since biasing leads to an implicit set of equations, a large matrix must be inverted. In KMRAD, this is done directly by Gaussian elimination. In practice, we have used timesteps ten or more times larger than those permitted by the Courant condition, with no bad side-effects.

KMRAD is written in the laboratory frame. In this frame, Maxwell's equations are formally self-adjoint, which simplifies the field solver. Also, the background plasma dynamics are given simply by $\underline{J}_p = \sigma \underline{E}$ for the collision dominated regime. In many beam calculations,¹⁻⁵ a Galilean transformation, $z' = z - Vt$, $t' = t$, where V is the beam velocity, is made. Under this transformation, Maxwell's equations lose their self-adjointness, and are more difficult to invert. In the interests of computational speed, we decided not to implement such a transformation in KMRAD.

D. Verification of KMRAD

KMRAD's algorithms have been subjected to many tests, both individually and as a whole. Here we describe the results of a test in which KMRAD was compared to the cold-fluid code GRADR.¹² GRADR computes the eigenmodes and eigenvalues of an arbitrary beam equilibrium (rather than solving an initial-value problem). Both codes were run for the case of a cold rotating monoenergetic beam with a step-function current profile, as shown in Fig. 1. The beam is in a channel with constant conductivity

throughout, and is 50% current neutralized. At $r = 1$, there is a conducting wall. When this problem is simulated using KMRAD, all unstable modes grow up from the initial kick given to the currents. Eventually, the most unstable mode dominates. In GRADR, on the other hand, individual modes are computed one at a time. In comparing the real and imaginary parts of the frequencies from the two codes in Table 1, we list only a few of the GRADR results. There are an infinite number of radial modes, and only those near maximum growth-rate are tabulated. The agreement between the two codes is better than 10%. We compare the radial profiles of the perturbed fields produced by the two codes in Fig. 2. The KMRAD profiles are superpositions of many modes, while only the most unstable mode from GRADR is depicted. Despite this, the profiles are qualitatively very similar (there is an arbitrary phase factor multiplying GRADR solutions). Only the most important fields are shown in Fig. 2, although all six components of \underline{E} and \underline{B} have nonzero amplitudes.

III. RESISTIVE INSTABILITIES ON BENNETT EQUILIBRIUM BEAMS

There is experimental evidence^{13,14} that self-pinch monoenergetic particle beams tend towards a Bennett distribution¹⁵ under the influence of multiple small-angle scattering. In this section, we look at the stability of the Bennett distribution with respect to resistive instabilities. Our primary purpose is to compare KMRAD with analytic models of these instabilities. The analytic models make some restrictive assumptions, and for our present purpose we shall also make them. Thus, the beam is assumed to be completely charge-neutral. The conductivity and return current density profiles are taken to be proportional to the beam current density profile. The conductivity profile is assumed to remain fixed as the beam oscillates. As far as we know, no attempt has been made to treat resistive modes with $m > 1$ analytically for Bennett beams. For m sufficiently large, one can neglect the radial inhomogeneity of the beam, and the problem is more tractable.¹⁶ In general, high m -number modes are unstable only for highly current-neutralized beams (neutralization fraction $f > 90\%$). As we shall see in subsection C, however, the $m = 2$ mode has a significant growth rate for $f = 80\%$. In what follows, we shall only consider the $m = 0, 1$, and 2 modes.

A. Axisymmetric Instabilities: $m = 0$

Lee² has modeled the sausage mode of a Bennett beam by assuming that the beam oscillations are self-similar, and by taking account of radial inhomogeneity through an "empirical" damping factor. Uhm and Lampe³ have modeled the instability more rigorously, but for a step-function current profile. The analysis of these models is done in a transformed coordinate system $z' = z - Vt$, $t' = t$. As a result, one obtains a dispersion relation solely in terms of the two dimensionless variables $(\omega - kV)/\omega_B$ and $\sigma\omega$, where ω_B is the betatron frequency. One then obtains the scaling laws $\omega - kV \propto \omega_B$ and $\omega \propto \sigma^{-1}$. Since KMRAD is written in the laboratory frame, it does not yield results in terms of these variables, but rather

in terms of ω/ω_B and kV/ω_B . The simple scaling laws are obscured, and the dispersion relation contains a "free parameter", namely $\alpha \equiv 4\pi\omega_B a^2/V^2$, where a is the beam radius. We note, however, that the scaling obtained analytically relies on several assumptions not made in KMRAD. In comparing KMRAD with the analytic models, we shall operate in a regime where these assumptions are, in fact, valid.

We illustrate the growth rates obtained from the analytic models and KMRAD in Fig. 3. In this figure, $\alpha = 55$. (Specifically we had in mind a 10 kA, 50 MeV beam with a Bennett radius of 0.3 cm in a channel with an on-axis conductivity of $4 \times 10^{12} \text{ sec}^{-1}$.) The beam is 80% current-neutralized. The radial field profiles from KMRAD are shown in Fig. 4. The code is rather noisy for nonlaminar equilibria. However, it is clear that the dominant mode is the lowest radial mode, the so-called breathing mode. The growth rate is considerably larger than that predicted by Lee's model. This may be due to an overestimate of the empirical damping factor in his model. The growth rate is lower than that obtained by Uhm and Lampe. It is to be expected that a beam with a rounded profile should give lower growth rates than one with a step-function profile because of the spread in betatron frequencies.

We computed the group velocity of the most unstable wavenumber to be about 0.7 c. Thus, in the beam frame, the instability will convect backwards and eventually reach the tail of the beam.

We have also looked at the case of a 40% current neutralized beam, and find it to be also unstable, but with the maximum growth rate reduced by about a factor of 4. We are unable to say whether instability persists at $f = 0$, as there is a weak numerical growth of noise in the code.

B. Hose Instability: $m = 1$

The hose instability has been studied for many years.¹⁷ It has a serious effect on a beam in that it displaces the center of mass of the beam sideways, deflecting it bodily from its initial path. Furthermore, our studies to date indicate that the hose is the most unstable resistive mode for self-pinch beams with return current fractions from 0 to 80% (we have not looked at higher fractions). The analytic models against which we compare KMRAD are again those of Lee⁴ and Uhm and Lampe.⁵ These two models are based on different plausibility arguments, but yield similar equations.

We compare the real and imaginary parts of the frequencies obtained from KMRAD with those from Lee's model in Fig. 5. We have chosen $\alpha = 55$ again. For $kc/\omega_B < 0.8$, the agreement in both parts of the frequency is quite good, about 10%. The code predicts a somewhat larger cut-off wavenumber for the instability than the analytic model. Due to the weak noise growth, however, we cannot say exactly where the growth rate goes through zero. For $f = 0$, the Uhm-Lampe model gives identical results to those of Lee's model (Lee treats only $f = 0$). For $f > 0$ the mode is more unstable than for $f = 0$, as we see from Fig. 6. It is clear from Fig. 7 (in which $f = 80\%$), that the lowest radial mode is the most unstable. The growth rates obtained from KMRAD at $f = 80\%$ are compared to those of the Uhm-Lampe model in Fig. 8. The analytic growth rates are 50% larger. It is difficult to pinpoint the origin of discrepancies between the code and the analytic models because of the nature of the derivations of the latter.

Thus far, we have assumed that the conductivity profile has the same width as the beam current density profile. Intuitively, one would suspect that broadening the conductivity profile would tend to stabilize the beam. To confirm this, we ran a case with $f = 0$ and increased the

"Bennett" radius of the conductivity profile by 33%, keeping the on-axis conductivity constant. As seen in Fig. 6, this decreases the growth rate by about 20%.

C. Resistive Instability with $m = 2$

The only analytical dispersion relations for $m = 2$ which we know of are for cold beams.¹ Rather than comparing our results with the cold model, we simply present our findings. The dispersion relation obtained for $\alpha = 55$ is shown in Fig. 9. At $f = 0.8$, the maximum growth rate is about 30% less than that for $m = 0$, and the group velocity is approximately $0.7c$. The field profile plots in Fig. 10 again show that it is the lowest radial mode which is growing fastest.

IV. STATUS AND FURTHER DEVELOPMENT OF KMRAD

A. Summary of Results to Date

In its present form, KMRAD can obtain the linear dispersion relation for resistive instabilities of any azimuthal mode number on an arbitrary beam equilibrium. We have used the code to look at cold beam equilibria and Bennett equilibria. The cold beam results agree well with results from the exact cold-fluid code GRADR. We have compared the Bennett results with available analytic models. For $m = 0$, we obtain growth rates significantly larger than those predicted by Lee's model.² Our $m = 1$ dispersion relation agrees well with analytic models^{4,5} for $kc/\omega_B < 0.8$ when the return current fraction f is zero. When $f = 80\%$, however, there is 50% disagreement. In all the cases we have looked at, we find that the lowest radial mode is the most unstable. In addition, we find that $m = 2$ growth rates are comparable to those for $m = 0$.

B. Future Work

The usefulness of KMRAD is at present restricted by lack of a general equilibrium solver. We plan to write such a code as soon as possible, making use of the MRC code ORBIT¹⁸ which solves the equilibrium Vlasov-Maxwell equations.

All the analytic models we referred to in Sec. III assume that the conductivity profile remains fixed as the beam oscillates. It has been suggested¹⁹ that effects from perturbation of the conductivity may be important in certain cases. We intend to incorporate the relevant expressions into KMRAD before using it in any further studies.

KMRAD is by no means restricted to looking at resistive instabilities. The Ohm's Law model for the background could be replaced by a

more complicated model derived from the fluid equations, or indeed by a second species of particles. We anticipate that the code will prove useful in the study of many varieties of beam and beam-plasma instabilities.

TABLE 1. Comparison between KMRAD and GRADR frequencies (real and imaginary parts) for $m = 1$ and $m = 2$ instabilities of the equilibrium shown in Fig. 1. Frequencies are in units of $3 \times 10^{10} \text{ sec}^{-1}$, k is in cm^{-1} .

<u>m</u>	<u>k</u>	<u>ω</u>	
		GRADR	KMRAD
1	0.1	(0.06, 0.03)	
		(0.10, 0.04)	(0.10, 0.04)
		(0.11, 0.04)	
		(0.13, 0.03)	
2	0.1	(0.10, 0.01)	
		(0.15, 0.04)	(0.15, 0.045)
		(0.17, 0.05)	
		(0.19, 0.04)	

REFERENCES

1. S. Weinberg, J. Math. Phys. 8, 614 (1967).
2. E. P. Lee, UCID-18940, Lawrence Livermore National Laboratory (1981).
3. H. S. Uhm and M. Lampe, Phys. Fluids 24, 1553 (1981).
4. E. P. Lee, Phys. Fluids 21, 1327 (1978).
5. H. S. Uhm and M. Lampe, Phys. Fluids 23, 1574 (1980).
6. T. P. Hughes and B. B. Godfrey, AMRC-R-285, Mission Research Corporation, Albuquerque, (1981).
7. J. P. Freidburg, R. L. Moore and C. W. Nielson, in Proc. Third Conference on Numerical Simulation of Plasmas, Stanford (1969).
8. J. A. Byers in Proc. Fourth Conference on Numerical Simulation of Plasmas, Naval Research Laboratory, Washington (1970).
9. A. Friedman, R. N. Sudan, and J. Denavit, J. Comp. Phys. 40 ??? (1981).
10. B. B. Godfrey, AMRC-N-138, Mission Research Corporation, Albuquerque, (1980).
11. B. B. Godfrey and B. C. Goplen, Bull. Am. Phys. Soc. 25, 854 (1980); AMRC-N-146, Mission Research Corporation, Albuquerque, (1980).
12. D. J. Sullivan and B. B. Godfrey, AMRC-R-309, Mission Research Corporation, Albuquerque (1981).
13. E. P. Lee, Phys. Fluids 19, 60 (1976).
14. C. Ekdahl and W. Bostick, AMRC-N-182, Mission Research Corporation, Albuquerque (1982).
15. W. H. Bennett, Phys. Rev. 45, 893 (1934).
16. R. F. Hubbard and D. A. Tidman, Phys. Rev. Lett. 41, 866 (1978).
17. M. N. Rosenbluth, Phys. Fluids 3, 932 (1960); C. L. Longmire (unpublished).
18. L. A. Wright and B. B. Godfrey, AMRC-R-249, Mission Research Corporation, Albuquerque (1980).
19. M. Lampe, remarks made at Beam Propagation Code Workshop, JAYCOR, Alexandria, March 23-24 (1982).

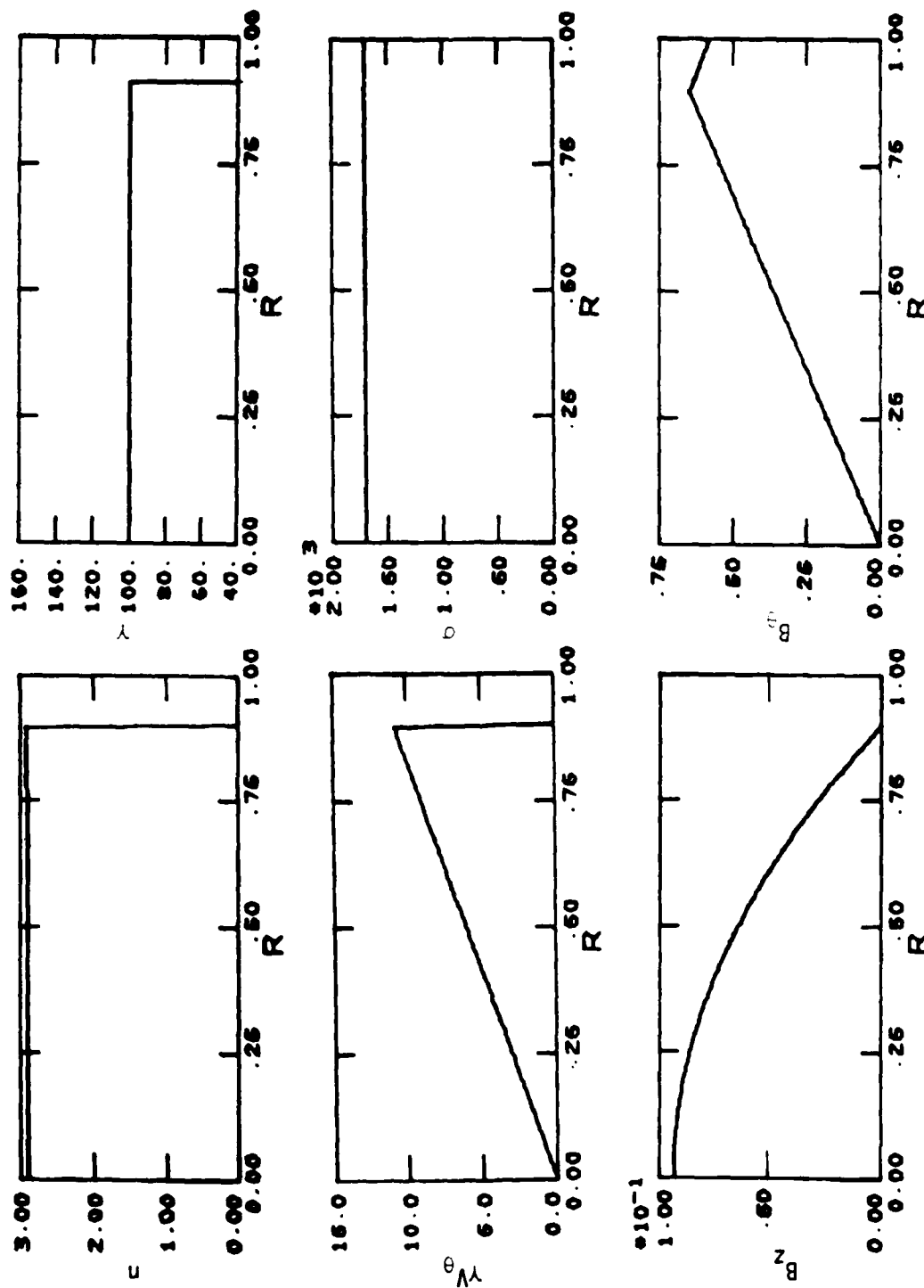


Figure 1. Cold beam equilibrium used to test KMRAD. Depicted are radial profiles of the density (n), energy (γ), angular velocity (γ_θ), conductivity (σ), axial and azimuthal magnetic fields (B_z , B_θ). The normalized units correspond to a 10 kA, 50 MeV beam with a radius of 0.9 cm. The beam is 50% current neutralized.

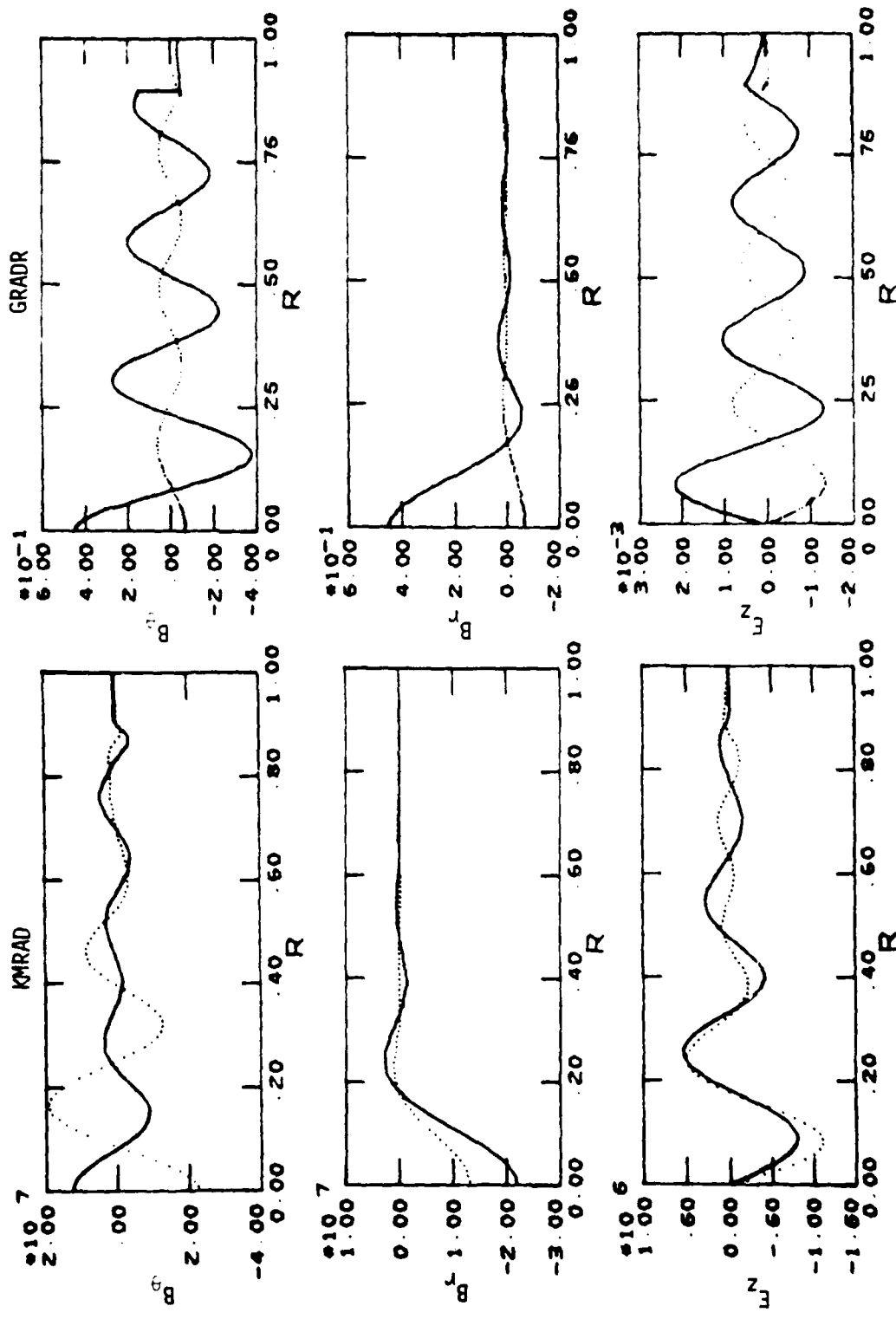


Figure 2(a). Radial profiles obtained from KMRAD and GRADR for the $m = 1$ instability. The GRADR mode with maximum growth rate is shown (see Table 1). Only the B_0 , B_z , E_z fields are shown since these are the most important. The solid and dotted lines indicate respectively the real and imaginary parts of each field.

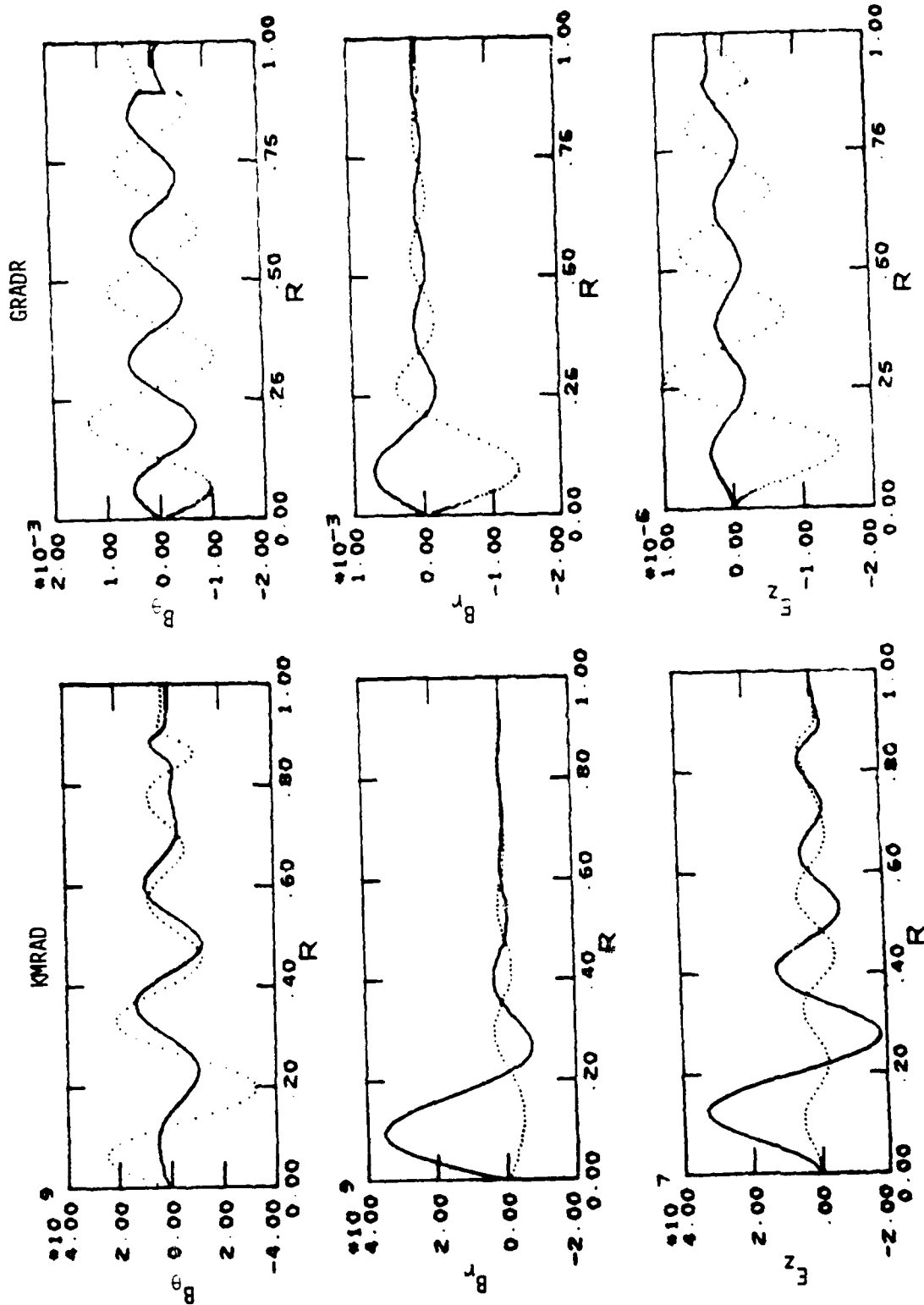


Figure 2(b). Radial profiles obtained from KMRAD and GRADR for the $m=2$ resistive instability. See Table 1.

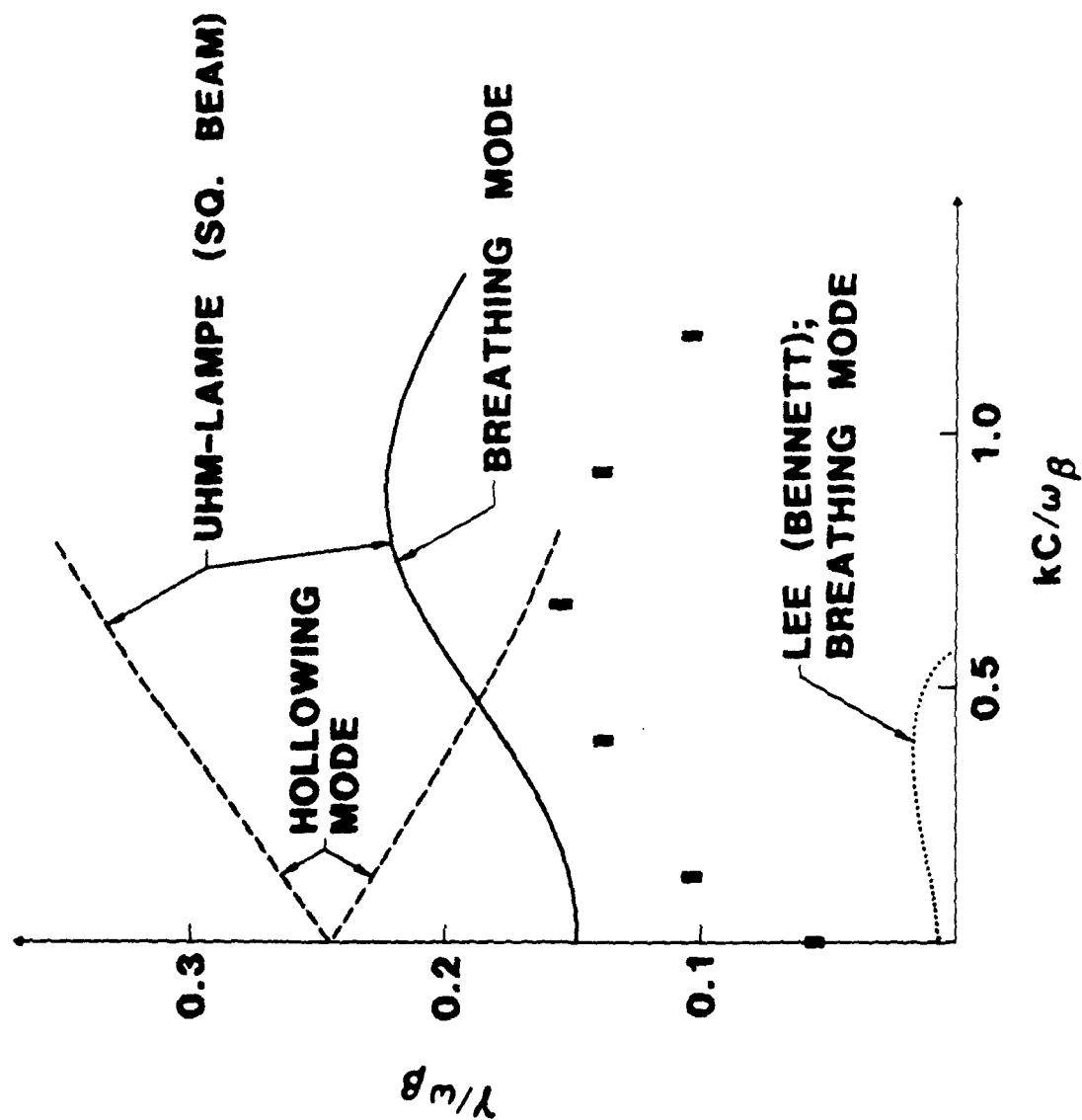


Figure 3. Comparison of growth rates for the $m = 0$ instability obtained from KMRAD (black rectangles) with those obtained from the analytic models of Lee and Uhm and Lampe. An 80% current neutralization fraction is assumed.

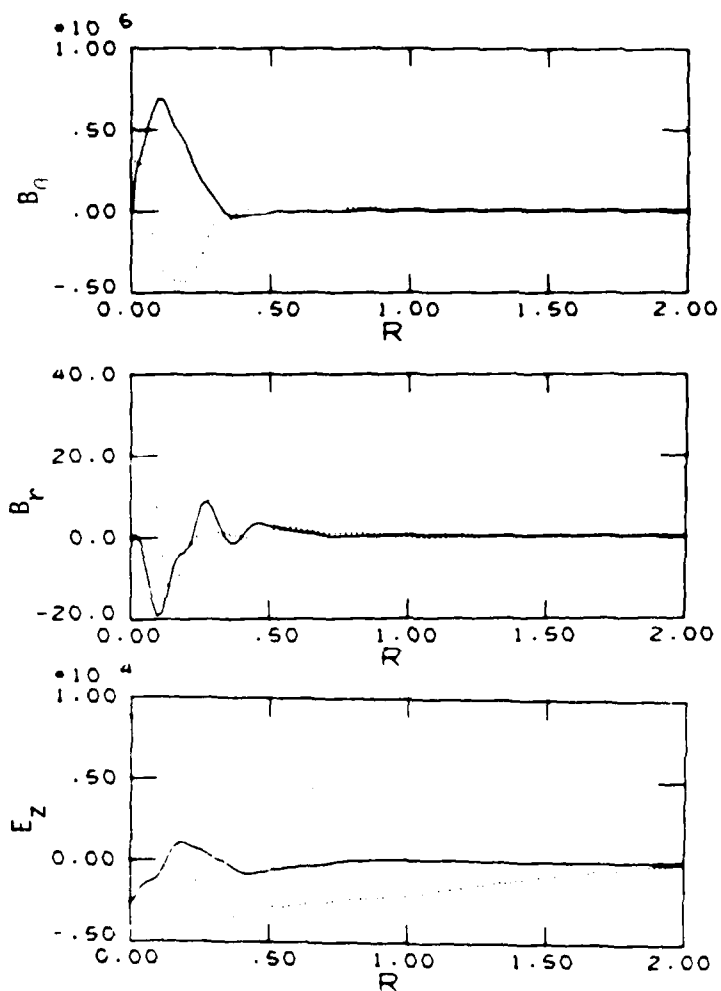


Figure 4. Radial profiles of the B_θ , B_r , E_z fields for the $m = 0$ mode, obtained from KMRAD. This mode corresponds to the value of k with the largest growth rate shown in Fig. 3.

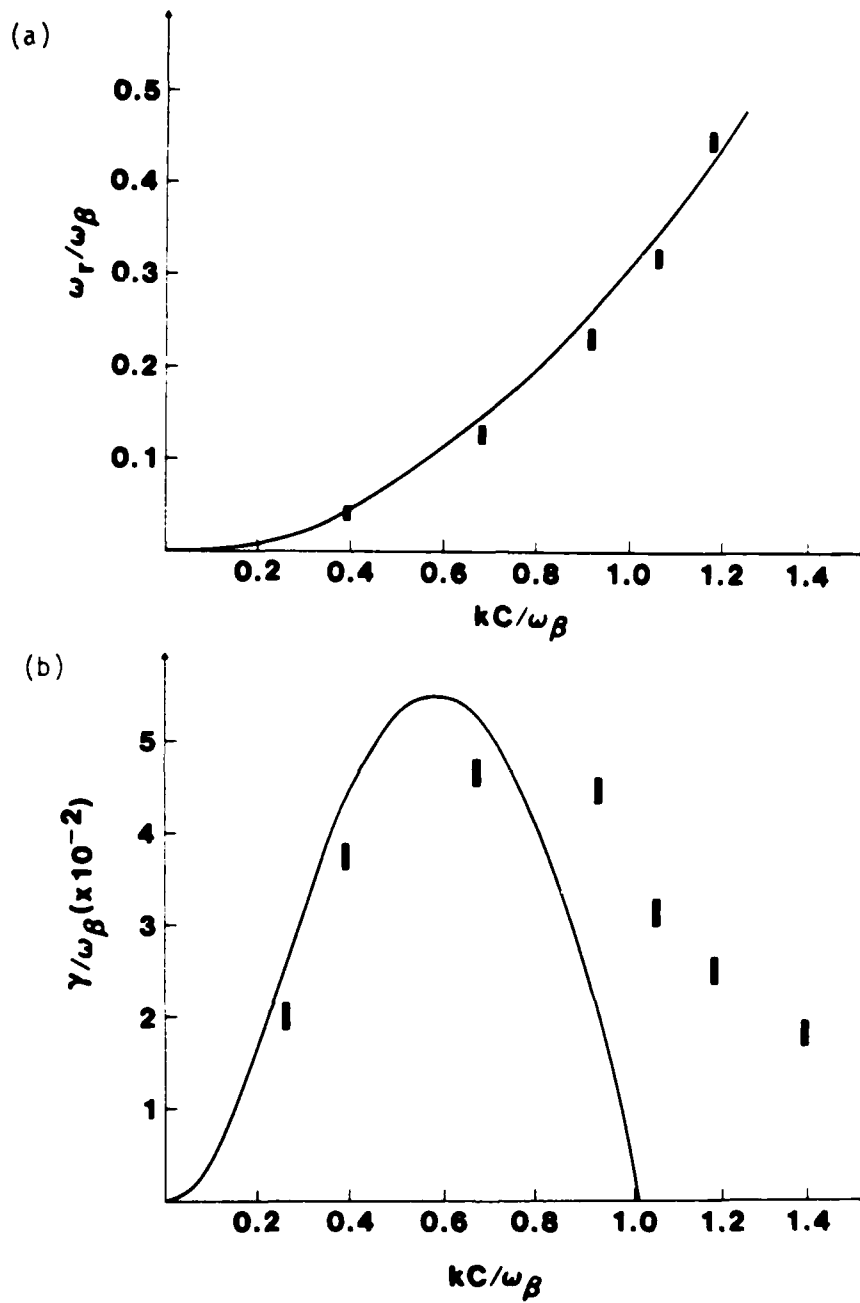


Figure 5. Comparison of the (a) real and (b) imaginary parts of the frequency of the $m = 1$ mode obtained from KMRAD, with those obtained from Lee's model. The beam has a Bennett equilibrium with no return current.

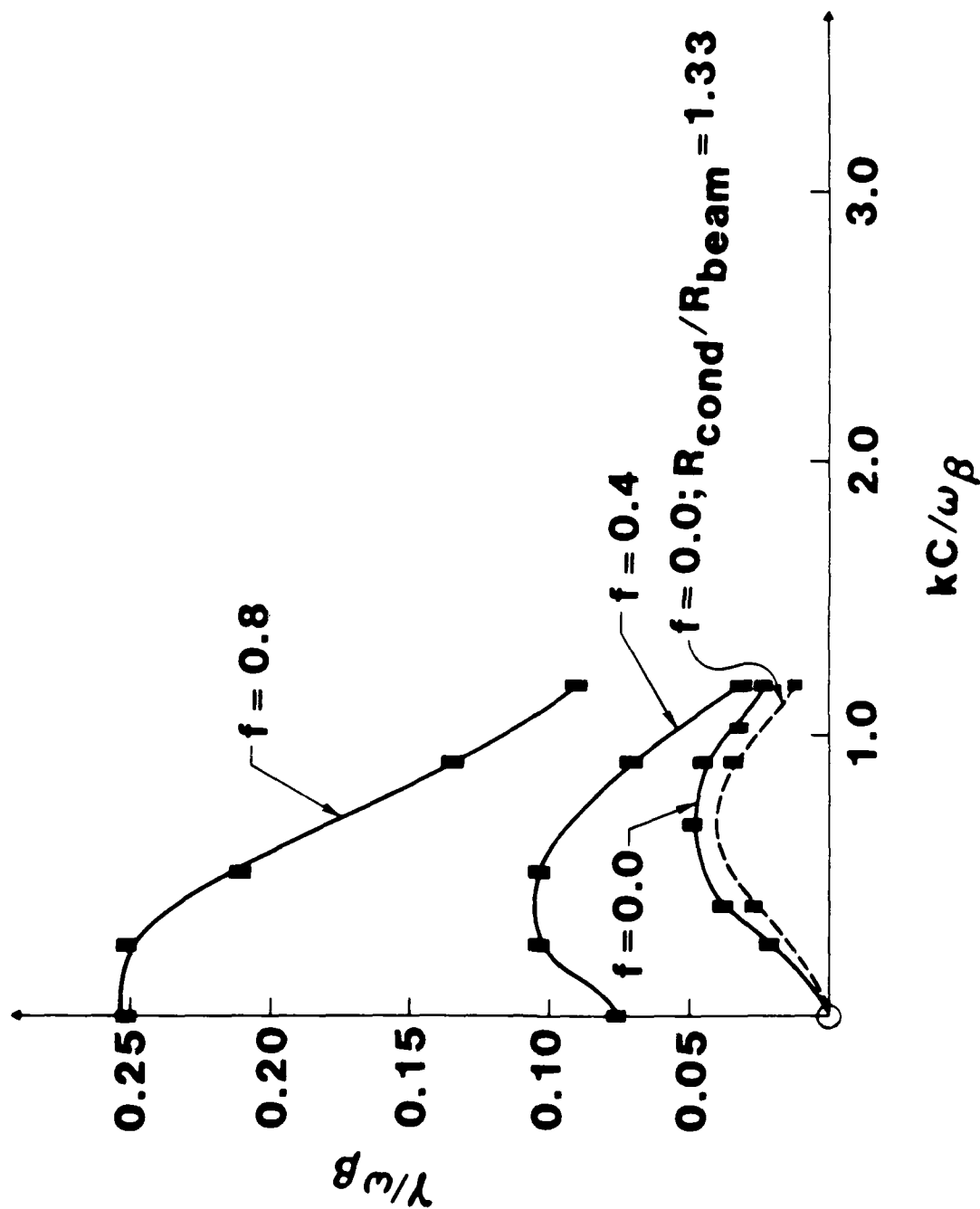


Figure 6. Growth rates of the $m = 1$ instability obtained from KMRAD for $f > 0$. We have connected the points for clarity. The dotted line shows results for a broadened conductivity profile.

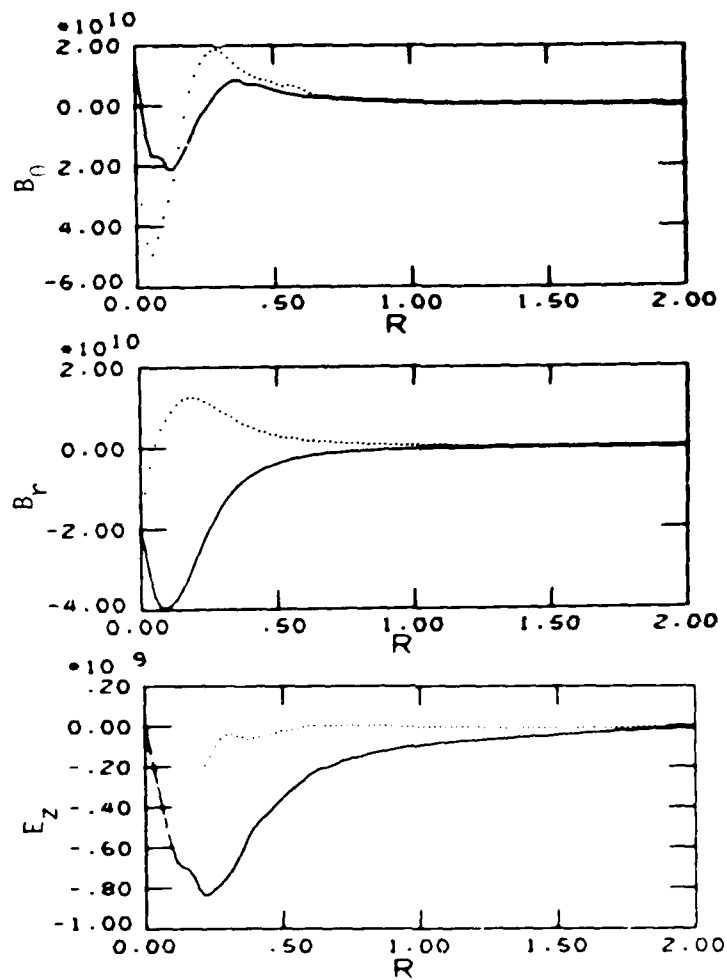


Figure 7. Radial profiles of B_0 , B_r , E_z for the $m = 1$ instability at $f = 80\%$, showing that the lowest radial mode is dominant.

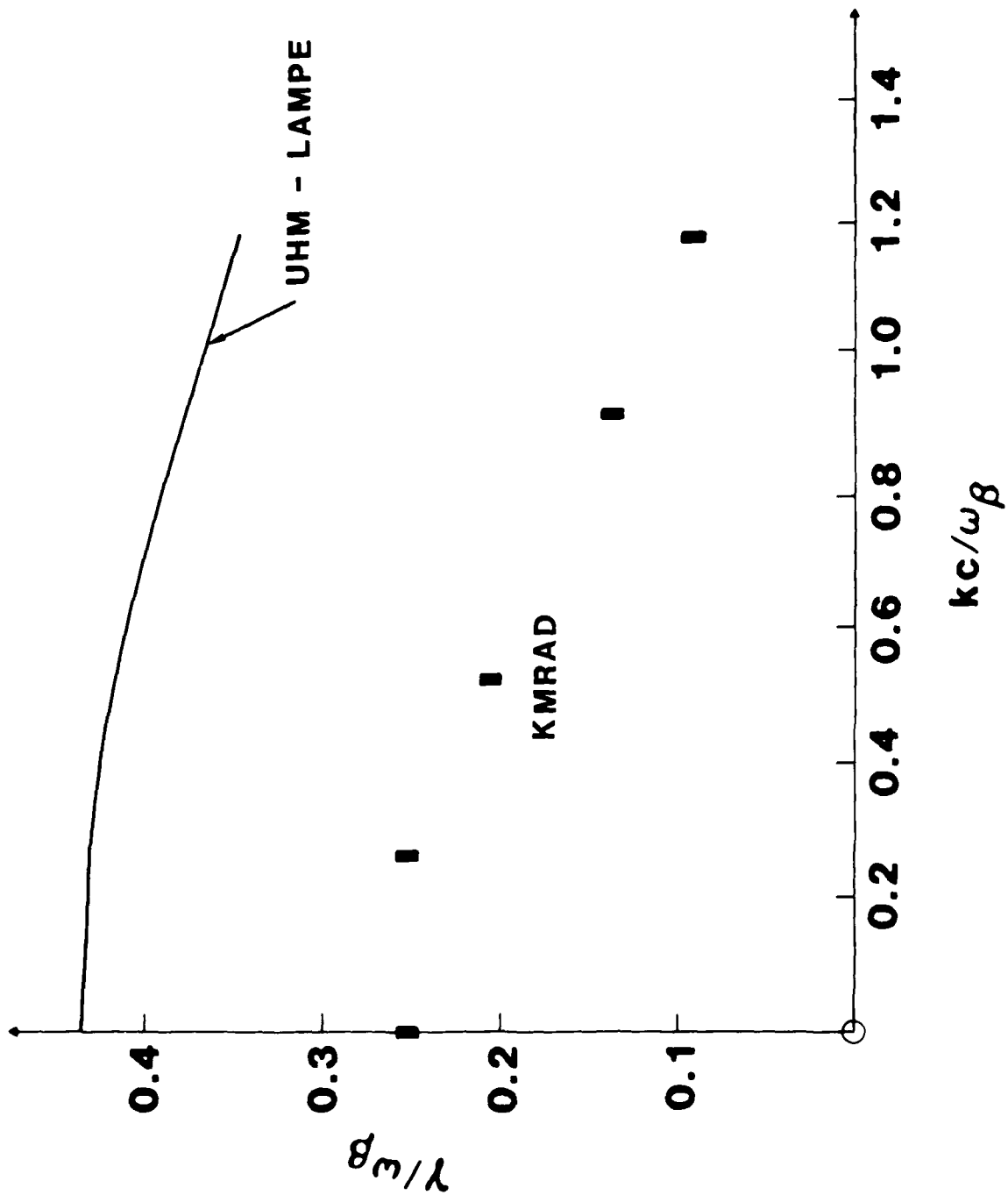


Figure 8. Comparison between the growth rates obtained from KMRAD for the $m = 1$ mode with those obtained from the Uhm-Lampe model. We assume $f = 80\%$.

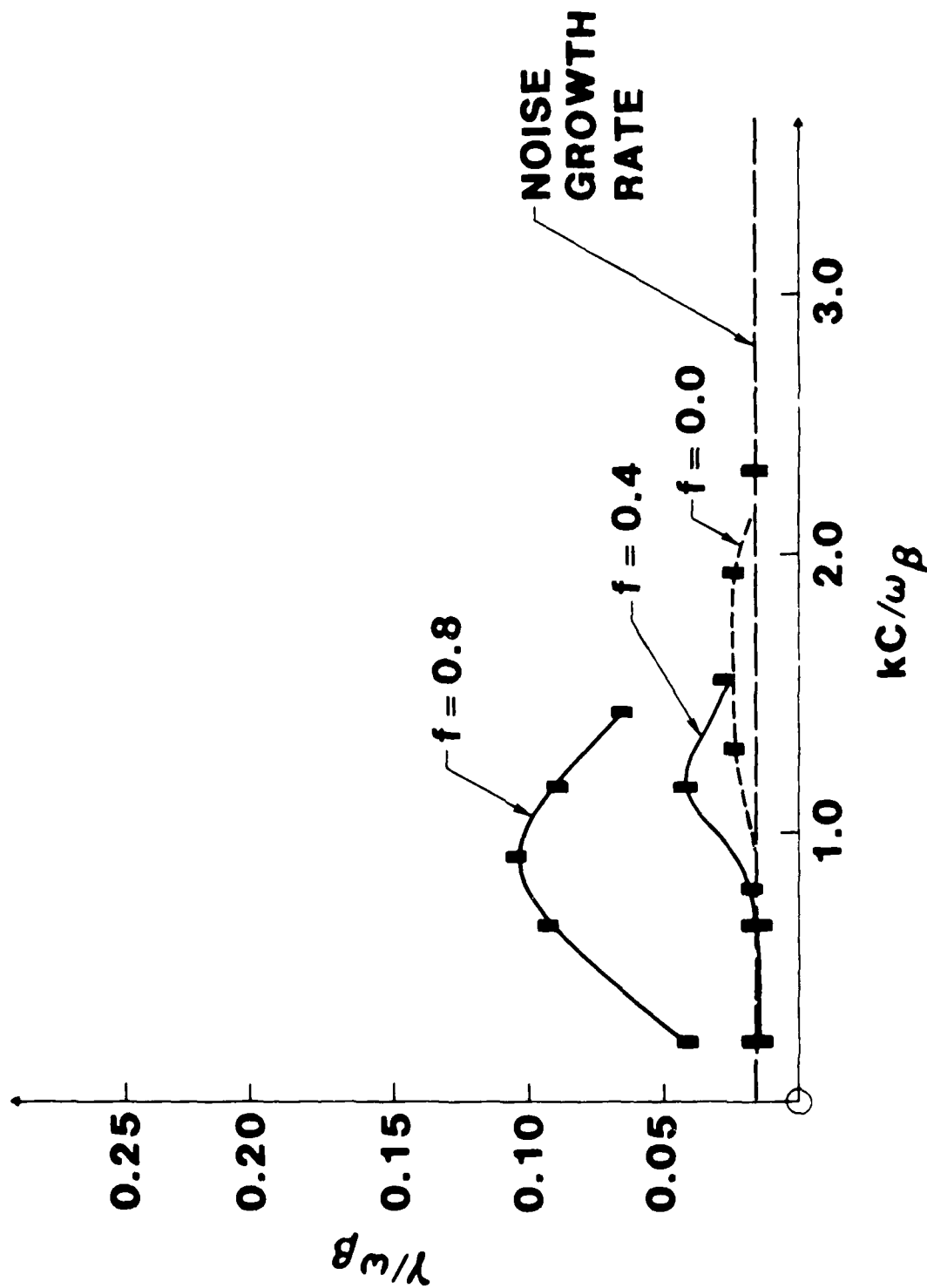


Figure 9. Growth rates of the $m = 2$ resistive instability computed by KMRAD for various current neutralization fractions. We have connected the points for clarity. There is a weak growth of noise in the code which does not allow us to see where the actual growth rate goes to zero.

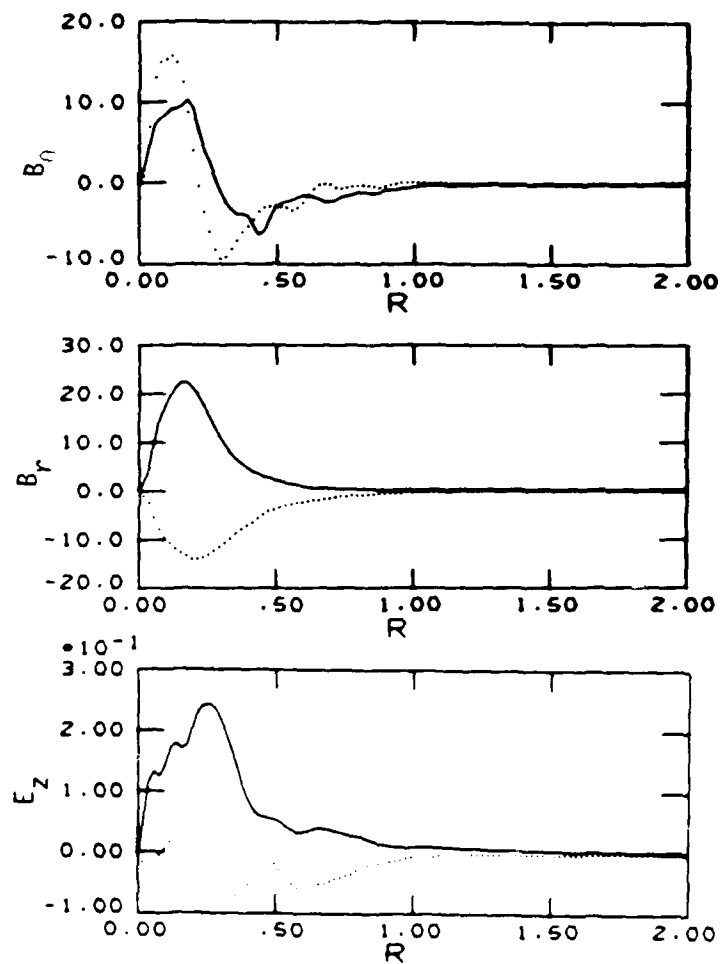


Figure 10. Radial profiles of the B_θ , B_r , E_z fields for the $m = 2$ instability at $f = 0.8$, illustrating the dominance of the lowest radial mode.